Scaling of Lipid Membrane Rigidity with Domain Area Fraction

Journal:	*Soft Matter*
Manuscript ID	SM-ART-11-2018-002362.R1
Article Type:	Paper
Date Submitted by the Author:	08-Feb-2019
Complete List of Authors:	Kelley, Elizabeth; National Institute of Standards and Technology, Center for Neutron Research Butler, Paul; National Institute of Standards and Technology; University of Delaware, Chemical and Biomolecular Engineering; The University of Tennessee, Knoxville, Department of Chemistry Nagao, Michihiro; NIST, NCNR; Indiana University, CEEM

SCHOLARONE™
Manuscripts

Soft Matter

ARTICLE TYPE

Scaling of Lipid Membrane Rigidity with Domain Area Fraction

Elizabeth G. Kelley,[*a] Paul D. Butler,[abc] and Michihiro Nagao[*ad]

Biological membranes are highly heterogeneous in composition which in turn leads to local variations in the physical properties. Here we quantify how heterogeneity in stiffness determines the effective bending modulus, κ_{eff}, of model phase-separated membranes with coexisting soft fluid and rigid gel domains. We find that the temperature- and composition- dependent trends in membrane rigidity collapse onto a single curve, such that κ_{eff} directly scales with the area fraction of the rigid gel domains. Using no adjustable parameters, the measurements are found to agree with theoretical predictions for inhomogenous membranes and indicate that κ_{eff} is sensitive to the lateral distribution of the rigid phase within the membrane. This key finding confirms that the properties of heterogeneous membranes can be quantitatively predicted if the area fraction and properties of the individual phases are known.

1 Introduction

The dynamics of soft membranes have attracted considerable theoretical and experimental attention for more than four decades. Much of this work has focused on lipid membranes as models for biological membranes, in which the underlying membrane dynamics and associated elastic properties influence both protein and cell functions. While significant advances have been made in quantifying the elastic properties of homogeneous membranes, much less is known about how the heterogeneity inherent in biological membranes affects their dynamics.

Biological membranes are a highly heterogeneous and crowded environment. Membranes contain rigid proteins and domains that are stiffer than the surrounding lipid matrix by a factor of 2 to 400.[1–8] Theoretical works that consider the effects of such rigid bodies, often referred to as inclusions or additives, show that the dynamics of heterogeneous membranes are governed by an effective bending modulus, κ_{eff}. The predicted deviations of κ_{eff} from the properties of homogeneous membranes are highly sensitive to the concentration, shape, and location of the inclusions, as well as whether inclusions are inserted or absorbed.[9–16] Further adding to the complexity, there are limited experimental data to compare with existing theories, and conflicting results show the inclusions can increase, decrease, or have a negligible
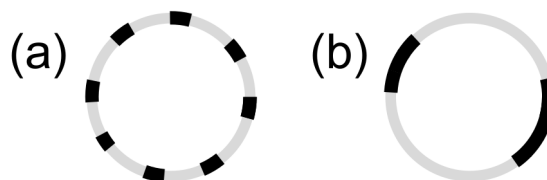

Fig. 1 Cartoon illustrations of lipid vesicle cross sections with (a) dispersed versus (b) aggregated domains.

effect on the membrane stiffness.[16–25]

Here, we study the particular case in which the rigid inclusions are embedded with the same average number density in each leaflet. In this case, simple mixing models predict that adding rigid inclusions will stiffen the membrane and that κ_{eff} will scale with ϕ, the area fraction of the rigid phase.[9–11] However, the theoretical work by Netz and Pincus also considers how the inclusions are organized within the membrane and predicts that the functional form of the κ_{eff} scaling with ϕ will depend on whether the domains are dispersed (Fig. 1a) or aggregated (Fig. 1b).[11] To the best of our knowledge, no experimental data span a wide enough concentration range of inclusions to compare with these differing theories. Comparisons between measurements and predictions at high ϕ, where the effects of the rigid phase on κ_{eff} are most pronounced, will reveal the importance of membrane lateral organization.

To test these predictions, we systematically quantify κ_{eff} in model heterogeneous membranes for a wide range of ϕ. We measure the bending undulations in phase-separated dimyristoylphosphocholine (DMPC, 14:0 PC) and distearylphospho-

[a] NIST Center for Neutron Research, National Institute of Standards and Technology, 100 Bureau Drive, Gaithersburg, MD, USA. E-mail: egk@nist.gov
[b] Department of Chemical and Biomolecular Engineering, University of Delaware, 150 Academy Street, Newark, DE, USA.
[c] Department of Chemistry, The University of Tennessee, Knoxville, TN 37996
[d] Center for Exploration of Energy and Matter, Indiana University, 2401 N. Milo B. Sampson Lane, Bloomington, IN, USA. E-mail: mnagao@indiana.edu

choline (DSPC, 18:0 C) membranes using neutron spin echo (NSE) spectroscopy. To vary ϕ from 0 to 1, we take advantage of the wide temperature range of two-phase coexistence by simply changing temperature in the phase coexistence region of the phase diagram (Fig. 2). Using no adjustable parameters, measurements of κ_{eff} as a function of ϕ show better agreement with the theory of Netz and Pincus for inhomogeneous membranes, demonstrating that the functional form of the scaling does indeed depend on the membrane lateral organization.

2   Experimental Section

2.1   Materials

Lipids were purchased from Avanti Polar Lipids and used without further purification. Deuterium oxide (D_2O, 99.9 % D) was purchased from Cambridge Isotopes. Relatively monodisperse unilameller vesicles with $\approx$ 100 nm diameter were prepared at the desired DMPC/DSPC ratios according to established extrusion protocols.[26,27] Lipids were mixed at the desired ratio in chloroform, dried under nitrogen, and then under vacuum overnight. The lipid film was rehydrated with D_2O at 55 °C to form multilayer vesicles. The multilayer vesicles then were sequentially extruded through 400 nm (15x), 200 nm (15x) and 100 nm (41x) and stored at 55 °C until measurement. The final solutions contained 100 mg/mL lipid in D_2O and were homogeneous by eye. Solutions were measured within 3 days of preparation. The sample stability was checked with dynamic light scattering (DLS) and small angle neutron scattering (SANS). SANS measurements were also used to confirm that > 95 % of the vesicles were unilameller (Fig. S1).

2.2   Differential Scanning Calorimetry (DSC)

DSC experiments were performed using a Microcal VP-DSC calorimeter. Samples were equilibrated at temperatures corresponding to the fluid phase, and at least 2 cooling and heating cycles were measured using a scan rate of 0.5 °C/min. The solvent background and baseline corrections were performed in the software package provided with the instrument,and the transition temperatures were determined using the tangent method (Fig. S2).[28] Samples for DSC experiments had a lipid concentration of 5 mg/mL.

2.3   Density Measurements

Density measurements were made using an Anton Paar DMA 500 density meter. The lipid volume was calculated from the measured density following procedures in literature.[29] The phase transition temperatures were determined from the derivative of the measured density versus temperature curve using the tangent method (Fig. S2).[28,30] Lipid samples for density measurements were diluted to 20 mg/mL.

2.4   Neutron Spin Echo Spectroscopy (NSE)

Data were collected on the NGA-NSE Spectrometer at the National Institute of Standards and Technology (NIST) Center for Neutron Research (NCNR) using neutron wavelengths (λ) of 0.8
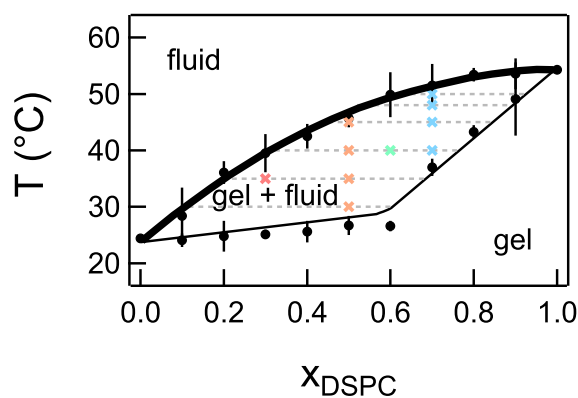

Fig. 2 Phase diagram for mixtures of DMPC/DSPC in D_2O constructed from densitometry and DSC experiments. The solid lines are the published phase diagram for DMPC/DSPC in H_2O shifted by +0.2 °C.[33] The bold line is referred to as the fluidus line and the dotted lines are the tie lines at the respective temperature. Crosses represent the temperatures measured with NSE for the different lipid mixtures. Error bars on the transition temperatures represent one standard deviation of measurements from different samples and different techniques. Error bars represent one standard deviation throughout the text and in some cases are smaller than the symbol.

nm and 1.1 nm with a wavelength spread of $\Delta\lambda/\lambda \approx 0.2$ to access a q-range of 0.45 nm^{-1} < q < 1.2 nm^{-1} and Fourier times, t, ranging from 0.01 ns to 100 ns corresponding to the nanoscale bending undulations.[31] The magnitude of the scattering vector, q, is defined as $q = 4\pi/\lambda \sin(\theta/2)$ in which θ is the scattering angle. The temperature was controlled within $\pm$ 0.5 °C and the samples were equilibrated for 30 min before starting the measurements. All data were collected on cooling. The NSE data were corrected for instrument resolution and D_2O solvent background to give the normalized intermediate scattering function $I(q,t)/I(q,0)$ using the DAVE software package.[32]

3   Results and Discussion

DMPC/DSPC mixtures are widely used as model systems to understand lipid membrane phase behavior and properties.[27,33–39] Our previous work measured the effects of the 4 carbon tail length mismatch on the dynamics of DMPC/DSPC mixtures in the fluid phase where the lipids are homogeneously mixed.[27] Here we focus on the membrane dynamics in the phase coexistence region. The phase behavior for DMPC/DSPC mixtures is well documented in literature; however, the NSE experiments required that the lipid mixtures be prepared in D_2O which is known to increase the melting transition temperature of pure lipids.[40] As seen in Fig. 2, our measurements of the lipid phase behavior using densitometry and differential scanning calorimetry (DSC) indicate that replacing H_2O with D_2O shifts the phase boundaries by $\approx$ 0.2 °C compared to the phase behavior reported for the mixtures in H_2O, but does not affect the shape of the boundaries. We refer to temperatures on the fluidus line as T_m, corresponding to the miscibility transition temperature.

The equilibrium bending undulations of the phase-separated membrane are governed by the effective elasticity, κ_{eff}. By directly measuring these thermal fluctuations with NSE, we are thus
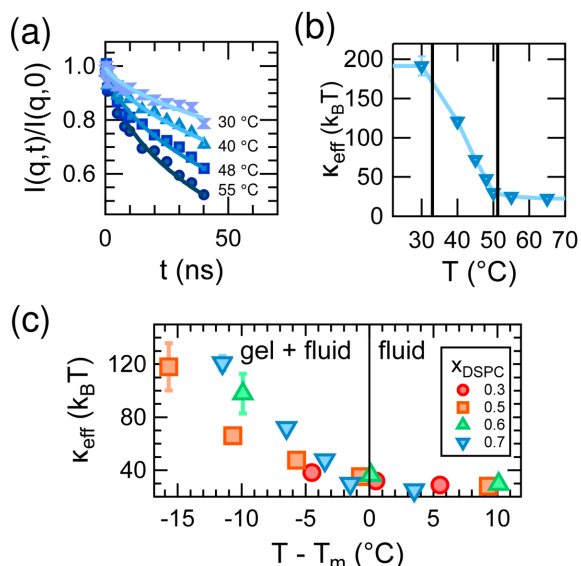
Fig. 3 (a) $I(q,t)/I(q,0)$ data (points) and fits to a stretched exponential (lines) at $q = 1.1$ nm^{-1} for indicated temperature and (b) corresponding values of κ_{eff} for mixed DMPC/DSPC membranes containing DSPC mole fraction (x_{DSPC}) of 0.7. The vertical lines in (b) demarcate the gel-fluid coexistence region. (c) Effective bending modulus, κ_{eff}, of mixed DMPC/DSPC lipid bilayers for the compositions given in the legend as a function of relative temperature, $T - T_m$, in which T_m corresponds to the temperatures on the fluidus line of the phase diagram.

able to study changes in κ_{eff} in the DMPC/DSPC bilayers as the mixtures are cooled from the fluid phase into the two-phase coexistence region and gel domains form. Shown in Fig. 3a are measured normalized intermediate scattering functions, $I(q,t)/I(q,0)$, for bilayers containing a DSPC mole fraction (x_{DSPC}) of 0.7 at temperatures corresponding to the fluid (55 °C), gel + fluid coexistence (48 °C and 40 °C), and gel phases (30 °C). As seen in the $I(q,t)/I(q,0)$ data in Fig. 3a, the relaxation time increases (curves decay less) with decreasing temperature, indicating that the membranes are becoming less dynamic (*i.e.* stiffer). All compositions exhibit this same behavior.

The $I(q,t)/I(q,0)$ data for all temperatures are well fit by a stretched exponential decay as expected for single membrane bending undulations described by Zilman and Granek,

$$I(q,t)/I(q,0) = \exp\left[-(\Gamma(q)t)^{2/3}\right] \tag{1}$$

in which $\Gamma(q)$ is relaxation rate.[41] The corresponding relaxation rates were used to determine the effective bending modulus, κ_{eff}, using refinements to the Zilman-Granek model made by Watson and Brown to account for the intermonolayer friction between leaflets according to

$$\Gamma = 0.0069 \frac{k_B T}{\eta} \sqrt{\frac{k_B T}{\kappa_{eff}}} q^3 \tag{2}$$

in which k_B is the Boltzman constant, T is the temperature, η is the viscosity of the D$_2$O solvent.[42,43]

The changes in the membrane stiffness as a function of temperature for $x_{DSPC} = 0.7$ are quantified as κ_{eff} in Fig. 3b. κ_{eff}

increases from ≈ 30 $k_B T$ in the fluid phase to ≈ 200 $k_B T$ in the gel phase of the mixed bilayers, consistent with the order of magnitude increase in bending moduli seen upon gelation of single component lipid bilayers.[30,44,45] However, the increase in modulus occurs over a much wider temperature range for the mixed DMPC/DSPC membranes than reported for single component bilayers. The bending modulus typically increases sharply at the melting temperature T_m of the lipid as expected for a first order transition in a single component membrane.[44,46,47] Here we see a gradual increase in κ_{eff} in all mixtures across the gel-fluid coexistence region of the phase diagram which can be up to 15 ° wide (Fig. 3c). Moreover, the gradual increase in κ_{eff} is not linear with temperature and its shape changes with composition in a non-intuitive fashion as evident from Fig. 3c.

According to theoretical works on heterogeneous membranes, the trends in κ_{eff} should scale in some way with the properties of the individual phases and their relative area fractions.[9–11] For a given lipid composition, the fraction of gel phase (f_{gel}) increases with decreasing temperature as the mixture is cooled into the coexistence region of the phase diagram. For a given temperature, f_{gel} will increase with increasing x_{DSPC} along the tieline. These trends in f_{gel} are qualitatively consistent with the changes in κ_{eff} with temperature and x_{DSPC} in Fig. 3c. The mole fraction of gel phase can be quantified from the phase diagram in Fig. 2 according to the lever rule and converted to the area fraction, ϕ, using published values for the area per lipid of phosphatidylcholine lipids in the fluid and gel phases. Here we take A$_{fluid} = 0.64$ nm^2 and A$_{gel} = 0.47$ nm^2, respectively.[48,49] We note that A$_{fluid}$ and A$_{gel}$ have a temperature dependence; however, these effects are expected to be at most a 5 % change and within the experimental uncertainty in the calculated ϕ value.[48–50] Replotting κ_{eff} as a function of ϕ (Fig. 4) collapses the data for all compositions onto a single master curve. In other words, the effective rigidity scales directly with the area fraction of gel phase as theoretically predicted.

The simplest expression for the effective rigidity was first given in works by Markin[9] and Helfrich and Kozlov[10] and predicts that κ_{eff} should follow a harmonic average of the fluid membrane and rigid inclusion moduli weighted by their respective area fractions,

$$\frac{1}{\kappa_{eff}} = \frac{\phi}{\kappa_{gel}} + \frac{1 - \phi}{\kappa_{fluid}} \tag{3}$$

in which κ_{gel} and κ_{fluid} are the bending moduli of the gel and fluid phases. Previous studies of both macroscopic and nanoscale phase separated membranes have shown that the coexisting phases have different moduli.[4–7] Assuming this behavior also holds in our systems, the bending moduli of the gel and fluid domains in a phase separated membrane are expected to be on the order of $\kappa_{fluid} \approx 30$ $k_B T$ and $\kappa_{gel} \approx 200$ $k_B T$, respectively. Corresponding values for κ_{eff} calculated using Eq. 3 are shown as the dotted line in Fig. 4. As seen in the plot, Eq. 3 systematically underestimates κ_{eff} for $\phi > 0.4$. Capturing the high ϕ data would require an unphysically large value of κ_{gel} on the order of 10^5 $k_B T$.

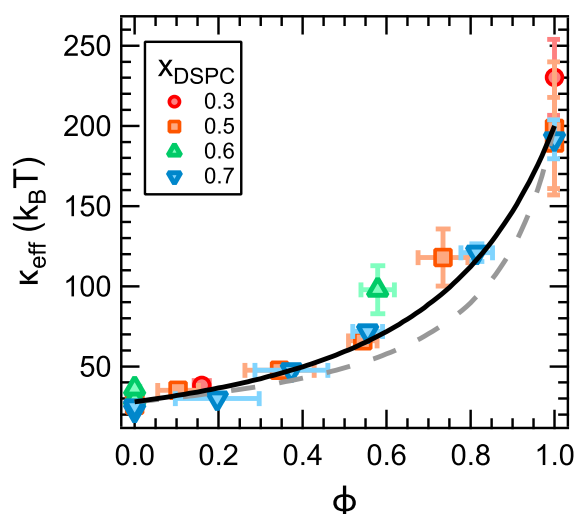More recent theoretical work by Netz and Pincus also pre-

Fig. 4 Effective bending modulus, κ_{eff}, as a function of the gel phase area fraction, ϕ, measured by NSE (points) and calculated from the gel and fluid phase moduli (lines). κ_{eff} was calculated using the averaged values of κ_{gel} = 202 k_BT and κ_{fluid} = 28 k_BT according to a weighted harmonic average (Eq. 3, dotted line, χ^2 = 18.7) and theory by Netz and Pincus (Eq. 4, solid line, χ^2 = 11.8) described in the text. Values in the legend refer to the membrane composition.

dict that κ_{eff} should follow Eq. 3 for membranes containing disordered and randomly mixed rigid inclusions as depicted in schematically in Fig. 1a. However, in the limit of an aggregated phase in which the membrane separates into a phase of close packed rigid inclusions and a phase of the pure fluid membrane such as in Fig. 1b, they instead predict

$$\frac{1}{\kappa_{eff}} = \left(\frac{\phi}{\sqrt{\kappa_{gel}}} + \frac{1-\phi}{\sqrt{\kappa_{fluid}}} \right)^2 \qquad (4)$$

Studies of phase-separated DMPC/DSPC mixtures indicate that the domains can be on the order of $\approx$ 100 nm in diameter and coarsen over time, and some works suggest that the gel phase can percolate forming a continuous phase.[37–39,51,52] Accordingly, Eq. 4 is expected to be a more appropriate model for the DMPC/DSPC membranes. Corresponding κ_{eff} values are plotted as the solid line in Fig. 4. Considering the solid line is not a fit, our experimental results are in remarkably good agreement with this prediction.

While the theories discussed here should apply to any rigid inclusions embedded in a soft surfactant or lipid membrane, how κ_{eff} scales with ϕ has direct implications for understanding the effects of transmembrane proteins on the stiffness of biological membranes. Red blood cells,[53] synaptic vesicles,[54] and viral membranes[55] have a transmembrane protein area occupancy on the order of $\approx$ 20 % to 30 %. Fig. 4 suggests that the rigid proteins may only have a small effect on κ_{eff} at physiological concentrations regardless of how the proteins are distributed in the membrane (solid versus dashed line). At ϕ = 0.2, the inhomogeneous membranes are $\approx$ 1.2 to 1.3 times stiffer than the bare fluid membrane from Eq. 3 and Eq. 4, respectively. These calculated values are for an $\approx$ 8x difference in moduli between the gel and fluid domains. Recent experimental results by Rosholm

et al. suggest that proteins are $\approx$ 1.6 times stiffer than the cell membrane, and the resulting κ_{eff} would be even smaller for this difference in moduli.[3] The predicted small increase is consistent with measurements of the mechanical properties of lipid extracts from the plasma membrane of red blood cells that showed the $\approx$ 20 % area occupancy of transmembrane proteins had no appreciable effect on the membrane flexibility.[21] However, incorporating more and/or stiffer protein would have a more significant effect. For example, Halobacterium halobium can incorporate as much as 75 % by mass of the protein bacteriorhodopsin into its purple membrane which would have a much greater effect on the membrane elasticity.[55]

The measured increase in κ_{eff} for phase-separated membranes at high ϕ is in good agreement with the scaling predicted by Netz and Pincus for inhomogeneous membranes with an aggregated rigid phase and shows that κ_{eff} does indeed depend on how the rigid phase is distributed in the membrane. The differences in the predicted scaling for aggregated versus dispersed rigid phases are most evident for $\phi > 0.4$ in Fig. 4. Our data follow Eq. 4 predicted for aggregated rigid inclusions, which is consistent with the formation of large gel domains reported in phase-separated DMPC/DSPC membranes. At the other limit of dispersed nanodomains or proteins, the theory predicts that κ_{eff} will instead follow a weighted harmonic average (Eq. 3). Work by Sigurdsson et al. found good agreement between κ_{eff} values from their simulations and calculated by Eq. 3 for proteins dispersed in a lipid bilayer for $\phi < 0.3$; however, the simulated values deviated from the theory for $0.3 < \phi < 0.5$, and simulations were not performed at higher ϕ.[2] While more experimental data are needed to validate the predictions for dispersed rigid phases, ongoing investigations into the effects of domain size, lipid chemistry, and other additives such as nanoparticles and proteins, will further elucidate the role of membrane composition and organization in determining κ_{eff}.

4   Conclusions

In summary, we quantified the effective elasticity of phase-separated DMPC/DSPC membranes and validated the theoretically predicted effects of rigid domains on κ_{eff} of inhomogeneous membranes. We showed that the data for different lipid mixing ratios and temperatures collapse onto a single master curve in which κ_{eff} directly scales with the area fraction of gel phase and properties of the fluid and gel phases in phase-separated membranes. Our data agreed with theoretical predictions of Netz and Pincus with no adjustable parameters and provide a framework for quantitatively understanding the effects of rigid inclusions, such as lipid domains and integral membrane proteins, on the membrane elasticity based on their number density and relative stiffness.

This work was designed to experimentally measure the effective rigidity for a specific case of inhomogenous membranes described by theory. As stated at the outset, biological membranes are highly complex and there are likely many contributions to κ_{eff}. For example, asymmetrically shaped inclusions, such as conical proteins like nicotinic acetylcholine receptors or potassium channels,[56,57] are predicted to couple to local curvature

and lead to membrane softening. [12–16] Moreover, several studies have shown that adding proteins can modify the local membrane structure which in turn influences the membrane rigidity. [17,25] Of course many proteins also are not perfectly rigid and their dynamics must also couple to the membrane dynamics. Nevertheless, we hope that the insights provided by these simple model systems will inform and inspire future measurements of the effects of compositional heterogeneity on the elasticity of more biologically-relevant lipid membranes and the interplay between the membrane mechanics and biological function.

5 Acknowledgements

References

1 T. A. Harroun, W. T. Heller, T. M. Weiss, L. Yang and H. W. Huang, *Biophys. J.*, 1999, **76**, 937–945.

2 J. K. Sigurdsson, F. L. H. Brown and P. J. Atzberger, *J. Comp. Phys.*, 2013, **252**, 65–85.

3 K. R. Rosholm, N. Leijnse, A. Mantsiou, V. Tkach, S. L. Pedersen, V. F. Wirth, L. B. Oddershede, K. J. Jensen, K. L. Martinez, N. S. Hatzakis, P. M. Bendix, A. Callan-Jones and D. Stamou, *Nat. Chem. Bio.*, 2017, **13**, 724.

4 T. Baumgart, S. T. Hess and W. W. Webb, *Nature*, 2003, **425**, 821.

5 T. Baumgart, S. Das, W. W. Webb and J. T. Jenkins, *Biophys. J.*, 2005, **89**, 1067–1080.

6 B. Kollmitzer, P. Heftberger, R. Podgornik, J. F. Nagle and G. Pabst, *Biophys. J.*, 2015, **108**, 2833–2842.

7 J. D. Nickels, X. Cheng, B. Mostofian, C. Stanley, B. Lindner, F. A. Heberle, S. Perticaroli, M. Feygenson, T. Egami, R. F. Standaert, J. C. Smith, D. A. A. Myles, M. Ohl and J. Katsaras, *J. Am. Chem. Soc.*, 2015, **137**, 15772–15780.

8 R. D. Usery, T. A. Enoki, S. P. Wickramasinghe, M. D. Weiner, W.-C. Tsai, M. B. Kim, S. Wang, T. L. Torng, D. G. Ackerman, F. A. Heberle, J. Katsaras and G. W. Geigenson, *Biophys. J.*, 2017, **112**, 720–731.

9 V. S. Markin, *Biophys. J.*, 1981, **36**, 1–19.

10 W. Helfrich and M. M. Kozlov, *J. Phys. II*, 1994, **4**, 1427–1438.

11 R. R. Netz and P. Pincus, *Phys. Rev. E*, 1995, **52**, 4114–4128.

12 J. B. Fournier, *Phys. Rev. Lett.*, 1996, **76**, 4436.

13 S. Leibler, *J. Physique*, 1986, **47**, 507–516.

14 S. Ramaswamy, J. Toner and J. Prost, *Phys. Rev. Lett.*, 2000, **84**, 3494.

15 E. Bivas and P. Méléard, *Phys. Rev. E*, 2003, **67**, 012901.

16 P. Girard, J. Prost and P. Bassereau, *Phys. Rev. Lett.*, 2005, **94**, 088102.

17 G. Pabst, S. Danner, R. Podgornik and J. Katsaras, *Langmuir*, 2007, **23**, 11705–11711.

18 H. Bouvrais, P. Meleard, T. Pott, K. J. Jensen, J. Braks and J. H. Ipsen, *Biophys. Chem.*, 2008, **137**, 7–12.

19 W. Rawicz, B. A. Smith, T. J. McIntosh, S. A. Simon and E. Evans, *Biophys. J.*, 2008, **94**, 4725–4736.

20 J.-H. Lee, S.-M. Choi, C. Doe, A. Faraone, P. A. Pincus and S. R. Kline, *Phys. Rev. Lett.*, 2010, **105**, 038101.

21 R. S. Gracia, N. Bezlyepkina, R. L. Knorr, R. Lipowsky and R. Dimova, *Soft Matter*, 2010, **6**, 1472–1482.

22 S. Tristram-Nagle, R. Chan, E. Kooijman, P. Uppamoochikkal, W. Qiang, D. P. Weliky and J. F. Nagle, *J. Mol. Biol.*, 2010, **402**, 139–153.

23 I. Hoffmann, R. Michel, M. Sharp, O. Holderer, M.-S. Appavou, F. Polzer, B. Farago and M. Gradzielski, *Nanoscale*, 2014, **6**, 6945–6952.

24 P. W. Fowler, J. Helie, A. Duncan, M. Chavent, H. Koldso and M. S. P. Sansom, *Soft Matter*, 2016, **12**, 7792–7803.

25 H. Agrawal, M. Zelisko, L. Liu and P. Sharma, *Sci. Rep.*, 2016, **6**, 25412.

26 A. C. Woodka, P. D. Butler, L. Porcar, B. Farago and M. Nagao, *Phys. Rev. Lett.*, 2012, **109**, 058102.

27 R. Ashkar, M. Nagao, P. D. Butler, A. C. Woodka, M. K. Sen and T. Koga, *Biophys. J.*, 2015, **109**, 106–112.

28 T. Heimburg, *Thermal Biophysics of Membranes*, WILEY-VCH Verlag GmbH & Co., Weinheim, Germany, 2007.

29 A. I. Greenwood, S. Tristram-Nagle and J. F. Nagle, *Chem. Phys. Lipids*, 2006, **143**, 1–10.

30 T. Heimburg, *Biochim. Biophys. Acta, Biomembranes*, 1998, **1415**, 147–162.

31 N. Rosov, S. Rathgeber and M. Monkenbusch, in *Neutron Spin Echo Spectroscopy at the NIST Center for Neutron Research*, American Chemical Society, 1999, vol. 739, book section 7, pp. 103–116.

32 R. T. Azuah, L. R. Kneller, Y. Qiu, P. L. W. Tregenna-Piggott, C. M. Brown, J. R. D. Copley and R. M. Dimeo, *J. Res. Natl. Inst. Stand. Technol.*, 2009, **114**, year.

33 S. Mabrey and J. M. Sturtevant, *Proc. Natl. Acad. Sci.*, 1976, **73**, 3862–3866.

34 W. Knoll, J. Haas, H. B. Stuhrmann, H.-H. Fuldner, H. Vogel and E. Sackmann, *J. Appl. Crystallogr.*, 1981, **14**, 191–202.

35 M. B. Sankaram, D. Marsh and T. E. Thompson, *Biophys. J.*, 1992, **63**, 340–349.

36 M. B. Sankaram and T. E. Thompson, *Biochemistry*, 1992, **31**, 8258–8268.

37 L. A. Bagatolli and E. Gratton, *Biophys. J.*, 2000, **79**, 434–447.

38 E. I. Michonova-Alexova and I. P. Sugár, *Biophys. J.*, 2002, **83**, 1820–1833.

39 E. Jens, P. P. Eugene and S. Petra, *New J. Phys.*, 2011, **13**,

045019.

40 S. A. Simon, L. J. Lis, J. W. Kauffman and R. C. Macdonald, *Biochimica et biophysica acta*, 1975, **375**, 317–326.

41 A. G. Zilman and R. Granek, *Phys. Rev. Lett.*, 1996, **77**, 4788–4791.

42 M. C. Watson and F. L. H. Brown, *Biophys. J.*, 2010, **98**, L9–L11.

43 M. Nagao, E. G. Kelley, R. Ashkar, R. Bradbury and P. D. Butler, *J. Phys. Chem. Lett.*, 2017, **8**, 4679–4684.

44 R. Dimova, *Adv. Colloid Interface Sci.*, 2014, **208**, 225–234.

45 D. Needham and E. Evans, *Biochemistry*, 1988, **27**, 8261–8269.

46 Z. Yi, M. Nagao and D. P. Bossev, *J. Phys.: Condens. Matter*, 2009, **21**, 155104.

47 C.-H. Lee, W.-C. Lin and J. Wang, *Phys. Rev. E*, 2001, **64**, 020901.

48 N. Kučerka, M.-P. Nieh and J. Katsaras, *Biochim. Biophys. Acta, Biomembranes*, 2011, **1808**, 2761–2771.

49 S. Tristram-Nagle, Y. Liu, J. Legleiter and J. F. Nagle, *Biophys. J.*, 2002, **83**, 3324–3335.

50 W. J. Sun, S. Tristram-Nagle, R. M. Suter and J. F. Nagle, *Biophys. J.*, 1996, **71**, 885–891.

51 W. L. Vaz, E. C. Melo and T. E. Thompson, *Biophys. J.*, 1989, **56**, 869–876.

52 C. Favard, J. Wenger, P.-F. Lenne and H. Rigneault, *Biophysical Journal*, 2011, **100**, 91242–1251.

53 A. D. Dupuy and D. M. Engelman, *Proc. Natl. Acad. Sci.*, 2008, **105**, 2848–2852.

54 S. Takamori, M. Holt, K. Stenius, E. A. Lemke, M. Grønborg, D. Riedel, H. Urlaub, S. Schenck, B. Brügger, P. Ringler, S. A. Müller, B. Rammner, F. Gräter, J. S. Hub, B. L. De Groot, G. Mieskes, Y. Moriyama, J. Klingauf, H. Grubmüller, J. Heuser, F. Wieland and R. Jahn, *Cell*, 2006, **127**, 831–846.

55 U. Coskun and K. Simons, *FEBS Lett.*, 2010, **584**, 1685–1693.

56 D. A. Doyle, J. Morais Cabral, R. A. Pfuetzner, A. Kuo, J. M. Gulbis, S. L. Cohen, B. T. Chait and R. MacKinnon, *Science*, 1998, **280**, 69–77.

57 N. Uniwn, *Journal of Molecular Biology*, 2005, **346**, 967–989.

Table of Contents Entry

for

Scaling of Lipid Membrane Rigidity with Domain Area Fraction

Elizabeth G. Kelley,* Paul D. Butler, and Michihiro Nagao*

Figure:
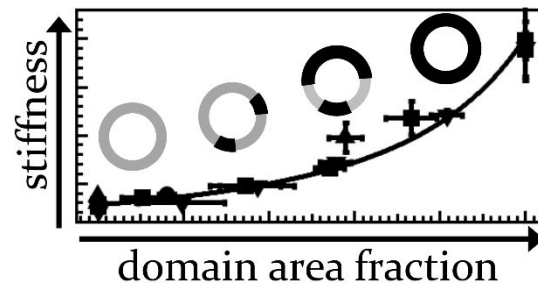
Sentence:

The effective rigidity of phase separated membrane scales according to theory with no adjustable parameters.